

Throughput Region of Spatially Correlated Interference Packet Networks

Alireza Vahid, Robert Calderbank

Abstract

In multi-user wireless packet networks interference, typically modeled as packet collision, is the throughput bottleneck. Users become aware of the interference pattern via feedback and use this information for contention resolution and for packet retransmission. Conventional random access protocols interrupt communication to resolve contention which reduces network throughput and increases latency and power consumption. In this work we take a different approach and we develop opportunistic random access protocols rather than pursuing conventional methods. We allow wireless nodes to communicate without interruption and to observe the interference pattern. We then use this interference pattern knowledge and channel statistics to counter the negative impact of interference. The result of our approach is better use of resources (*e.g.*, time and energy) and higher network throughput. We prove the optimality of our protocols using an extremal rank-ratio inequality. An important part of our contributions is the integration of spatial correlation in our assumptions and results. We identify spatial correlation regimes in which inherently outdated feedback becomes as good as idealized instantaneous feedback, and correlation regimes in which feedback does not provide any throughput gain.

Index Terms

Wireless packet networks, random-access protocol, interference management, spatial correlation, correlation across users, network throughput, communication protocol, erasure interference channel, delayed CSIT, capacity region.

I. INTRODUCTION

Recent years have seen a dramatic increase in wireless data traffic thanks to new paradigms such as heterogeneous networks and device-to-device communications. But perhaps more important than the increase in data traffic, is the fact that the character of wireless communications is changing. We are experiencing a transition from a wireless world with human users to one with machines. In this new wireless world we need to accommodate coexistence over the same band of a massive number of communicating machines. However, this task is quite challenging as it is hard to predict when these machines wish to communicate. Moreover, the interference environment constantly changes and at the time of communication, we may not know what this environment looks like. These challenges demand new solutions beyond the conventional medium-access protocols.

Conventional random-access protocols such as ALOHA [2] and ALOHA-type mechanisms interrupt communication to resolve contention. This interruption will result in long silent periods in massive machine-type communication (mMTC) which will reduce network throughput and will increase latency. In low-power wide-area networks (LP-WANs), the interruption will result in more retransmission and increased power consumption. Both these scenarios are undesirable. One approach to mitigate this problem is to add more and more signaling in order to allow users to come to an agreement and share the medium, but this approach comes at the cost of further payload reduction.

In this work we take a different approach and we develop *open-loop opportunistic communication protocols*. We allow wireless nodes to communicate without interruption and to observe the interference pattern. We then use this interference pattern knowledge and channel statistics to counter the negative impact of interference. The result of our approach is better use of resources (*e.g.*, time and energy) and higher network throughput. More precisely, we consider a wireless packet network with multiple transmitter-receiver pairs and within this network, we focus

Alireza Vahid is with the Department of Electrical Engineering, University of Colorado Denver, Denver, CO, USA. Email: alireza.vahid@ucdenver.edu.

Robert Calderbank is with departments of Electrical and Computer Engineering, Mathematics, and Computer Science, Duke University, Durham, NC, USA. Email: robert.calderbank@duke.edu.

Preliminary results of this work were presented at the 2016 IEEE International Symposium on Information Theory (ISIT) [1].

on two nearby pairs. We develop an opportunistic random-access or communication protocol for this network that updates the status of previously communicated packets based on the observed interference pattern. These packets are then combined and retransmitted efficiently through the medium. We also prove the optimality of our proposed scheme by developing an extremal rank-ratio inequality.

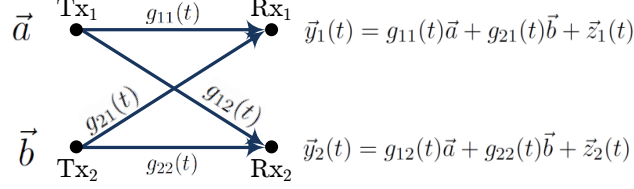


Fig. 1. At time t , Tx_1 and Tx_2 communicate data packets \vec{a} and \vec{b} respectively. $\vec{z}_1(t)$ and $\vec{z}_2(t)$ capture the ambient interference plus noise power.

We adopt the physical layer model for wireless packet networks introduced in [3] that allows the flexibility of storing the analog received signals at the receivers so that they can be utilized for decoding packets in the future. In this model the impact of interference from nearby users is captured by binary shadowing coefficients as described below. Suppose transmitters Tx_1 and Tx_2 communicate data packets \vec{a} and \vec{b} respectively at time t as in Fig. 1. Then receiver Rx_1 obtains

$$\vec{y}_1(t) = g_{11}(t)\vec{a} + g_{21}(t)\vec{b} + \vec{z}_1(t), \quad (1)$$

where $g_{11}(t)$ and $g_{21}(t)$ are real-valued channel gains and $\vec{z}_1(t)$ is the ambient interference plus noise power. In the physical layer model of [3] this received signal is represented by

$$\vec{y}_1(t) = \alpha_{11}(t)g_{11}(t)\vec{a} + \alpha_{21}(t)g_{21}(t)\vec{b}, \quad (2)$$

where the shadowing coefficients $\alpha_{11}(t)$ and $\alpha_{21}(t)$ are in the binary field and depend on the signal-to-interference-plus-noise ratios (SINRs) of different links and determine the interference pattern. This model is closely related to Erasure Interference Channel [4], [5] which in turn is a generalization of Erasure Broadcast Channel [6]–[10] to capture interference.

In this work, we assume wireless nodes learn the binary quadruple

$$\alpha(t) = (\alpha_{11}(t), \alpha_{12}(t), \alpha_{21}(t), \alpha_{22}(t)) \quad (3)$$

with unit delay. This model is commonly referred to as delayed channel state information at the transmitters or delayed CSIT for short.

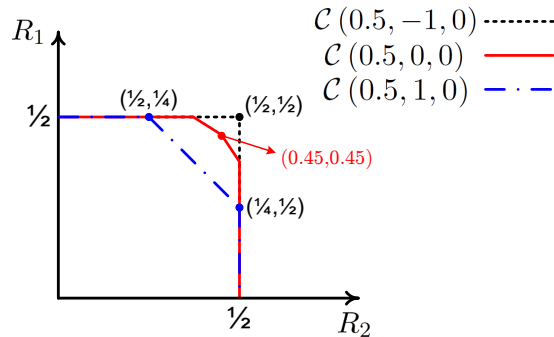


Fig. 2. Throughput region for $B(0.5)$ shadowing coefficients and three different correlation coefficient pairs.

In most prior work fading coefficients are assumed to be independently and identically distributed across *time* and *space*. There are recent results on temporal correlation in wireless networks but there is very little known about spatial correlation. Here, we incorporate spatial correlation into our setting. We assume that there is a certain spatial correlation between these binary shadowing coefficients and that this knowledge is available to all nodes as side information. We show that spatial correlation can greatly affect the throughput region of wireless packet networks: spatial correlation on the one hand can take away any potential gain of delayed interference pattern knowledge and on the other hand, it can help us perform as well as having instantaneous knowledge of interference pattern. To see this dichotomy, we focus on the case in which all shadowing coefficients in (3) are distributed as Bernoulli $\mathcal{B}(0.5)$ random variables and assume that the coefficients corresponding to the wireless links connected to each receiver are distributed independently. When the two channels connected to each transmitter are fully correlated (*i.e.* correlation coefficient of 1), the throughput region $\mathcal{C}(0.5, 1, 0)$ coincides with the one where transmitters do not have any access to interference pattern knowledge as shown in Fig. 2. At the other extreme point where the two channels connected to each transmitter have a correlation coefficient of -1 , the gain of delayed interference pattern is accentuated and the throughput region $\mathcal{C}(0.5, -1, 0)$ is as good as the throughput region of a network in which a genie informs wireless nodes of the interference pattern before it even happens.

To derive the outer-bounds on the throughput region that capture spatial correlation of the channels, we develop an extremal rank-ratio inequality. We show that this inequality is tight and can be achieved. We then use genie-aided arguments and apply our extremal rank-ratio inequality to derive the outer-bounds. The slope of these outer-bounds is determined by the correlation coefficient at each transmitter. On the receiver side, correlation coefficients determine the size of the available subspace at each receiver. In other words, spatial correlation at the transmitter side defines the shape of the throughput region while spatial correlation at the receiver side determines its size.

To achieve the outer-bounds, we develop an opportunistic communication that updates the status of each transmitted packet into three queues: 1) delivered packets, 2) packets that arrived (and potentially interfered) at both receivers; and 3) packets that arrived (and potentially interfered) at the unintended receivers. The protocol then combines the packets in the latter two queues taking into account the spatial correlation structure of the network. These combined packets will be transmitted efficiently through the medium and upon completion of the communication protocol, each receiver will have sufficient number of equations to recover its intended packets.

As mentioned above, there is a large body of work on wireless networks with delayed knowledge of the interference pattern or the channel state information. This delayed knowledge was used in [6] to create transmitted signals that are simultaneously useful for multiple users in a broadcast channel (BC). These ideas were then extended to different wireless networks, including erasure broadcast channels [8], [10] leading to determination of the Degrees of Freedom (DoF) region of multiple input single output (MISO) Gaussian BCs [11]. Approximate capacity of MISO BCs was presented in [12]. The DoF region of multi-antenna multi-user Gaussian interference channels (ICs) and X channels has been also considered [13]–[21], as well as the capacity region of Erasure ICs with delayed knowledge [4], [5].

Other results consider more realistic settings in which wireless links exhibit some sort of correlation. Temporal correlation has been studied in several papers [22]–[27] with the idea being that correlation across time allows transmitters to better estimate what will happen next, and to adjust their transmission strategies accordingly. In the context of broadcast channels, there are several results that propose transmission strategies that take into account spatial correlation of wireless links [28]–[31]. In the context of interference channels, a transmission strategy was developed in [32] for multiple input multiple output (MIMO) ICs with *instantaneous* channel knowledge and spatial correlation. However, a fundamental understanding of the throughput region of spatially correlated interference channels is missing and is the main focus of this work.

The rest of the paper is organized as follows. In Section II we formulate our problem and justify the physical layer model. In Section III we present our main results and provide some insights. Sections IV and V are dedicated to the proof of the main results. We describe connections to two related directions in Section VI, and Section VII concludes the paper.

II. PROBLEM FORMULATION

We consider a wireless packet network in which multiple transmitter-receiver pairs wish to communicate with each other and within this setup, we focus on two nearby transmitter-receiver pairs, namely T_{x1} - R_{x1} and T_{x2} - R_{x2} as depicted in Fig. 3.

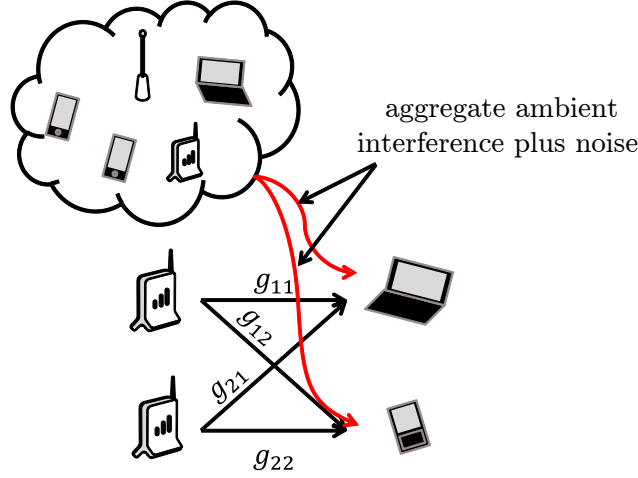


Fig. 3. A wireless packet network in which multiple transmitter-receiver pairs communicate with each other. We focus on two nearby pairs.

We adopt the abstraction for wireless packet networks introduced in [3]. In this model transmitter T_{x_1} has m_1 packets with corresponding physical layer codewords of length τ denoted by $\vec{a}_1, \vec{a}_2, \dots, \vec{a}_{m_1}$ and wishes to communicate them to receiver R_{x_1} . Similarly, transmitter T_{x_2} has m_2 packets denoted by $\vec{b}_1, \vec{b}_2, \dots, \vec{b}_{m_2}$ for receiver R_{x_2} . It is assumed that the mapping from the packets to their corresponding physical layer codewords is fixed (e.g., LDPC codes, Reed-Solomon codes, etc) and if a codeword is received with a signal-to-interference-plus-noise ratio of above γ , the receiver is able to decode its packet. The signal-to-interference-plus-noise ratio of link ji at R_{x_i} , $i, j \in \{1, 2\}$, is defined as:

$$\text{SINR}_{ji} \triangleq 10 \log_{10} \left(\frac{P|g_{ji}|^2}{\mathbb{E} [\vec{z}_i^T(t) \vec{z}_i(t)] + P|g_{\bar{j}i}|^2} \right), \quad (4)$$

where P is the average transmit power constraint and $\vec{z}_i(t)$ is noise plus the ambient interference power (from potential nearby transmitters except for T_{x_j}). Furthermore, we define the signal-to-noise ratio (SNR) of link ji at R_{x_i} , $i, j \in \{1, 2\}$, as:

$$\text{SNR}_{ji} \triangleq 10 \log_{10} \left(\frac{P|g_{ji}|^2}{\mathbb{E} [\vec{z}_i^T(t) \vec{z}_i(t)]} \right). \quad (5)$$

Based on SINR and SNR values of different links at each time t , we have one of the following states at any of the receivers, say R_{x_1} :

- State 1 ($\text{SINR}_{11} \geq \gamma$): In this state the SINR of the desired packet (i.e. \vec{a}) at R_{x_1} is above the threshold. Fig. 4(a) depicts this scenario.
- State 2 ($\text{SINR}_{21} \geq \gamma$): Similar to State 1, but in this case the SINR of the interfering packet (i.e. \vec{b}) at R_{x_1} is above the threshold and R_{x_1} (the unintended receiver in this case) can decode this packet, see Fig. 4(b).
- State 3 ($\text{SINR}_{i1} < \gamma$ but $\text{SNR}_{i1} \geq \gamma$ for $i = 1, 2$): This state corresponds to the scenario in which the SINRs of both packets (\vec{a} and \vec{b}) are below the threshold at R_{x_1} but the individual links are strong. Thus, receiver R_{x_1} obtains a linear combination of the packets as depicted in Fig. 4(c). In this case, the receiver cannot decode the packets. However, it stores the signal as the weighted linear combination of packets \vec{a} and \vec{b} .
- State 4: In any other scenario, R_{x_1} discards the received signal, see Fig. 4(d).

The following abstraction of the physical layer at R_{x_1} captures the four different states:

$$\vec{y}_1(t) = \alpha_{11}(t)g_{11}(t)\vec{a} + \alpha_{21}(t)g_{21}(t)\vec{b}, \quad (6)$$

where the shadowing coefficients $\alpha_{ij}(t)$'s are in the binary field, $i, j \in \{1, 2\}$. For example in State 3 we have $(\alpha_{11}(t) = 1, \alpha_{21}(t) = 1)$ and

$$\vec{y}_1(t) = g_{11}(t)\vec{a} + g_{21}(t)\vec{b}. \quad (7)$$

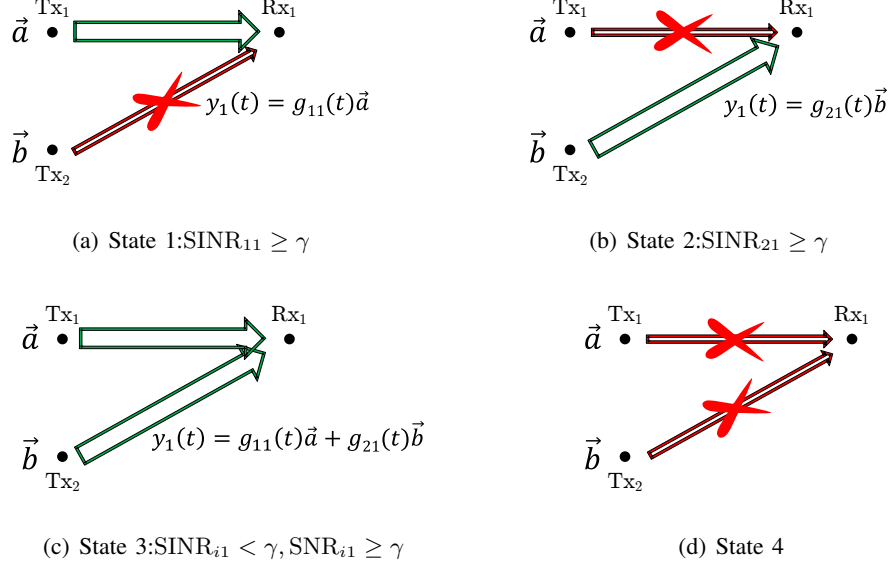


Fig. 4. Based on the SINR and SNR values of different links at each time t , we have four states.

Similarly, $\alpha_{12}(t)$ and $\alpha_{22}(t)$ can be used for Rx_2 .

The channel-state at time instant t is represented by quadruple

$$\alpha(t) = (\alpha_{11}(t), \alpha_{12}(t), \alpha_{21}(t), \alpha_{22}(t)). \quad (8)$$

We assume that $\alpha_{ij}(t)$ follows a Bernoulli distribution $\mathcal{B}(p)$ and that at time t , each transmitter knows $\alpha^{t-1} = (\alpha(\ell))_{\ell=1}^{t-1}$ and each receiver has access to $\alpha^t = (\alpha(\ell))_{\ell=1}^t$.

In general, $\alpha_{ji}(t)$'s are correlated across time and space. As mentioned in the introduction, correlation across time allows us to predict the future and improve the throughput that way. On the other hand, there is little known about spatial correlation and that is the focus of the current paper. Since we study the impact of spatial correlation, in this work we assume that $\alpha_{ij}(t)$'s are distributed independently across time and are drawn from the same joint distribution at each time. To capture spatial correlation, we assume a symmetric setting in which the shadowing coefficients corresponding to the links connected to transmitter Tx_i have a correlation coefficient ρ_{Tx} , *i.e.*

$$\rho_{\text{Tx}} = \frac{\text{cov}(\alpha_{i1}(t), \alpha_{i2}(t))}{\sigma_{\alpha_{i1}(t)} \sigma_{\alpha_{i2}(t)}}, \quad i = 1, 2. \quad (9)$$

and the links connected to receiver Rx_j have a correlation coefficient ρ_{Rx} , *i.e.*

$$\rho_{\text{Rx}} = \frac{\text{cov}(\alpha_{1j}(t), \alpha_{2j}(t))}{\sigma_{\alpha_{1j}(t)} \sigma_{\alpha_{2j}(t)}}, \quad j = 1, 2. \quad (10)$$

We note that fixing $-1 \leq \rho_{\text{Tx}}, \rho_{\text{Rx}} \leq 1$ imposes a feasible set on p . More precisely, we require p to be in $\mathcal{S}_{\rho_{\text{Tx}}} \cap \mathcal{S}_{\rho_{\text{Rx}}}$ where $\mathcal{S}_{\rho_{\text{Tx}}}$ and $\mathcal{S}_{\rho_{\text{Rx}}}$ are defined below. First, we define

$$\begin{aligned} p_{ij}^{\text{Tx}} &\triangleq \Pr(\alpha_{11}(t) = i, \alpha_{12}(t) = j), \\ p_{ij}^{\text{Rx}} &\triangleq \Pr(\alpha_{11}(t) = i, \alpha_{21}(t) = j), \quad i, j \in \{0, 1\}, \end{aligned} \quad (11)$$

then, $\mathcal{S}_{\rho_{\text{Tx}}} \subseteq [0, 1]$ is the set of all values for p such that

$$\begin{cases} 0 \leq p_{00}^{\text{Tx}}, p_{10}^{\text{Tx}}, p_{01}^{\text{Tx}}, p_{11}^{\text{Tx}} \leq 1 \\ p_{10}^{\text{Tx}} + p_{11}^{\text{Tx}} = p \\ p_{01}^{\text{Tx}} + p_{11}^{\text{Tx}} = p \\ \sum_{i,j \in \{0,1\}} p_{ij}^{\text{Tx}} = 1 \\ pq\rho_{\text{Tx}} = p_{11}^{\text{Tx}}p^2 + (p_{01}^{\text{Tx}} + p_{10}^{\text{Tx}})pq + p_{00}^{\text{Tx}}q^2 \end{cases} \Rightarrow \begin{cases} p_{11}^{\text{Tx}} = pq\rho_{\text{Tx}} + p^2 \\ p_{10}^{\text{Tx}} = p - pq\rho_{\text{Tx}} - p^2 \\ p_{01}^{\text{Tx}} = p - pq\rho_{\text{Tx}} - p^2 \\ p_{00}^{\text{Tx}} = 1 - p_{11}^{\text{Tx}} - p_{10}^{\text{Tx}} - p_{01}^{\text{Tx}} \end{cases} \quad (12)$$

Similarly, $\mathcal{S}_{\rho_{\text{Rx}}} \subseteq [0, 1]$ is the set of all values for p such that

$$\begin{cases} 0 \leq p_{00}^{\text{Rx}}, p_{10}^{\text{Rx}}, p_{01}^{\text{Rx}}, p_{11}^{\text{Rx}} \leq 1, \\ p_{10}^{\text{Rx}} + p_{11}^{\text{Rx}} = p, \\ p_{01}^{\text{Rx}} + p_{11}^{\text{Rx}} = p, \\ \sum_{i,j \in \{0,1\}} p_{ij}^{\text{Rx}} = 1, \\ pq\rho_{\text{Rx}} = p_{11}^{\text{Rx}}p^2 + (p_{01}^{\text{Rx}} + p_{10}^{\text{Rx}})pq + p_{00}^{\text{Rx}}q^2. \end{cases} \Rightarrow \begin{cases} p_{11}^{\text{Rx}} = pq\rho_{\text{Rx}} + p^2 \\ p_{10}^{\text{Rx}} = p - pq\rho_{\text{Rx}} - p^2 \\ p_{01}^{\text{Rx}} = p - pq\rho_{\text{Rx}} - p^2 \\ p_{00}^{\text{Rx}} = 1 - p_{11}^{\text{Rx}} - p_{10}^{\text{Rx}} - p_{01}^{\text{Rx}} \end{cases} \quad (13)$$

We can write $\mathcal{S}_{\rho_{\text{Tx}}}$ and $\mathcal{S}_{\rho_{\text{Rx}}}$ as

$$\begin{aligned} \mathcal{S}_{\rho_{\text{Tx}}} &\triangleq \left[\max \left\{ 0, \frac{-\rho_{\text{Tx}}}{1 - \rho_{\text{Tx}}} \right\}, \min \left\{ 1, \frac{1}{1 - \rho_{\text{Tx}}} \right\} \right], \\ \mathcal{S}_{\rho_{\text{Rx}}} &\triangleq \left[\max \left\{ 0, \frac{-\rho_{\text{Rx}}}{1 - \rho_{\text{Rx}}} \right\}, \min \left\{ 1, \frac{1}{1 - \rho_{\text{Rx}}} \right\} \right], \end{aligned} \quad (14)$$

where we set $\mathcal{S}_{\rho_{\text{Tx}}=1}, \mathcal{S}_{\rho_{\text{Rx}}=1} \triangleq [0, 1]$.

Consider the scenario in which Tx_i wishes to reliably communicate m_i packets¹ to Rx_i during n uses of the channel, $i = 1, 2$. We assume that the packets and the channel gains are *mutually* independent. Receiver Rx_i is only interested in packets from Tx_i , and it will recover (decode) them using the received signal \bar{y}_i^n , the knowledge of the channel state information, and the knowledge of ρ_{Tx} and ρ_{Rx} .

At each time instant, transmitter i creates a linear combination of the m_i packets it has for receiver i by choosing a precoding vector $\vec{v}_i(t) \in \mathbb{R}^{1 \times m_i}$, $i = 1, 2$. Transmit signals at time t at Tx_1 and Tx_2 are given by $\vec{v}_1(t)\mathbf{A}$ and $\vec{v}_2(t)\mathbf{B}$ respectively, where $\mathbf{A} = [\vec{a}_1, \vec{a}_2, \dots, \vec{a}_{m_1}]^\top$, and $\mathbf{B} = [\vec{b}_1, \vec{b}_2, \dots, \vec{b}_{m_2}]^\top$. We impose the following constraints on $\vec{v}_1(t)$ and $\vec{v}_2(t)$ to satisfy the power constraint (*i.e.* an average transmit power of P) at the transmitters:

$$\|\vec{v}_1(t)\|, \|\vec{v}_2(t)\| \leq 1, \quad (15)$$

where $\|\cdot\|$ represents the Euclidean norm. Since transmitters learn $\alpha(t)$ with unit delay, $\vec{v}_i(t)$ is only a function of α^{t-1} and the correlation coefficients ρ_{Tx} and ρ_{Rx} . The received signal of receiver i at time t can be represented by

$$\bar{y}_i(t) = \alpha_{1i}(t)g_{1i}(t)\vec{v}_1(t)\mathbf{A} + \alpha_{2i}(t)g_{2i}(t)\vec{v}_2(t)\mathbf{B}. \quad (16)$$

We denote the overall precoding matrix of transmitter i by $\mathbf{V}_i^n \in \mathbb{R}^{n \times m_i}$, where the t^{th} row of \mathbf{V}_i^n is $\vec{v}_i(t)$. Furthermore, let \mathbf{G}_{ij}^n be an $n \times n$ diagonal matrix where the t^{th} diagonal element is $\alpha_{ij}(t)g_{ij}(t)$, $i, j = 1, 2$. Thus, we can write the output at receiver i as

$$\bar{y}_i^n = \mathbf{G}_{1i}^n \mathbf{V}_1^n \mathbf{A} + \mathbf{G}_{2i}^n \mathbf{V}_2^n \mathbf{B}, \quad i = 1, 2. \quad (17)$$

We denote the interference subspace at receiver i by \mathcal{I}_i and is given by

$$\mathcal{I}_i \triangleq \text{colspan}(\mathbf{G}_{ii}^n \mathbf{V}_i^n), \quad i = 1, 2, \quad (18)$$

where colspan of a matrix represents the sub-space spanned by its column vectors. Let \mathcal{I}_i^c denote the subspace orthogonal to \mathcal{I}_i . Then in order for decoding to be successful at receiver i , it should be able to create m_i linearly independent equations that are solely in terms of its intended packets. Mathematically speaking, this means that the image of $\text{colspan}(\mathbf{G}_{ii}^n \mathbf{V}_i^n)$ on \mathcal{I}_i^c should have the same dimension as $\text{colspan}(\mathbf{V}_i^n)$ itself. More precisely, we require

$$\dim(\text{Proj}_{\mathcal{I}_i^c} \text{colspan}(\mathbf{G}_{ii}^n \mathbf{V}_i^n)) = \dim(\text{colspan}(\mathbf{V}_i^n)) = m_i, \quad i = 1, 2. \quad (19)$$

We say that a throughput tuple of $(R_1, R_2) = (m_1/n, m_2/n)$ is achievable, if there exists a choice of \mathbf{V}_1^n and \mathbf{V}_2^n , such that (19) is satisfied for $i = 1, 2$ with probability 1. The throughput region, $\mathcal{C}(p, \rho_{\text{Tx}}, \rho_{\text{Rx}})$, is the closure of all achievable throughput tuples (R_1, R_2) . We note that the unit for R_i is packets per channel use.

¹We note that in this paper we assume transmitters start with a number of packets to communicate rather than stochastic arrival of packets.

III. STATEMENT OF THE MAIN RESULTS

The following theorem establishes the throughput region of spatially correlated interference packet networks with two transmitter-receiver pairs.

Theorem 1. *For the spatially correlated interference packet network with two transmitter-receiver pairs as described in Section II and for $p \in \mathcal{S}_{\rho_{\text{Tx}}} \cap \mathcal{S}_{\rho_{\text{Rx}}}$, we have*

$$\mathcal{C}(p, \rho_{\text{Tx}}, \rho_{\text{Rx}}) = \left\{ \begin{array}{ll} 0 \leq R_i \leq p, & i = 1, 2, \\ R_i + \beta(p, \rho_{\text{Tx}}) R_i \leq \beta(p, \rho_{\text{Tx}}) (1 - p_{00}^{\text{Rx}}), & i = 1, 2. \end{array} \right\} \quad (20)$$

where

$$\begin{aligned} \beta(p, \rho_{\text{Tx}}) &= 2 - \rho_{\text{Tx}} - p(1 - \rho_{\text{Tx}}), \\ p_{00}^{\text{Rx}} &= 1 + p^2 + pq\rho_{\text{Rx}} - 2p. \end{aligned} \quad (21)$$

Remark 1. *We would like to point out a subtle point regarding our problem formulation here. Fixing p, ρ_{Tx} , and ρ_{Rx} does not specify a unique channel but rather a family of channels as we only fix pairwise correlation coefficients at each node. For this family of channels, the throughput region is identical and given in Theorem 1. For more discussion on Bernoulli random variables with known pairwise correlations, we invite the reader to refer to [33].*

The converse proof of Theorem 1 relies on an extremal rank-ratio inequality for correlated channels that we present in Section IV. The slope of the outer-bounds (i.e. $\beta(p, \rho_{\text{Tx}})$ in the theorem) is determined by this inequality and depends on spatial correlation at the transmitters. Using the extremal inequality and genie-aided arguments, we obtain the outer-bound.

The communication protocol has multiple phases of communications and after each phase, transmitters use the delayed interference pattern knowledge to update the status of the previously communicated packets. The goal is to retransmit linear combinations of packets in a way to help receivers decode their corresponding packets faster than the case in which individual packets are retransmitted.

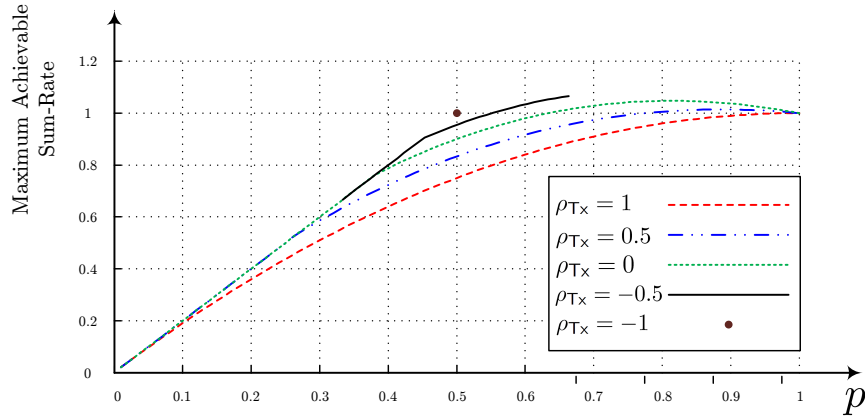


Fig. 5. Maximum achievable sum-rate for $\rho_{\text{Tx}} \in \{-1, -0.5, 0, 0.5, 1\}$, $\rho_{\text{Rx}} = 0$, and $p \in \mathcal{S}_{\rho_{\text{Tx}}} \cap \mathcal{S}_{\rho_{\text{Rx}}}$.

Before presenting the proofs, we provide further interpretation of Theorem 1. We first focus on the impact of correlation at the transmitters on the throughput region. Note that since $\alpha_{ij}(t)$'s are distributed as $\mathcal{B}(p)$, the maximum throughput we can expect in this network is $2p$. Fig. 5 depicts the maximum achievable sum-rate for $\rho_{\text{Tx}} \in \{-1, -0.5, 0, 0.5, 1\}$, $\rho_{\text{Rx}} = 0$ (i.e. independent links at the receivers), and $p \in \mathcal{S}_{\rho_{\text{Tx}}}$. For a fixed value of p as ρ_{Tx} moves from $+1$ to -1 , the maximum achievable sum-rate improves. In fact, for $p = 0.5$ as discussed in the introduction and shown in Fig. 2, $\mathcal{C}(0.5, 1, 0)$ coincides with the one where transmitters do not have any access to interference pattern [3]. On the other hand, $\mathcal{C}(0.5, -1, 0)$ includes $(R_1, R_2) = (0.5, 0.5)$ which implies that the throughput region coincides with the throughput region of a network in which a genie informs wireless nodes of the interference pattern before it even happens. Intuitively, this is due to the fact that with fully correlated

channels, each transmitter cannot distinguish between the two receivers and as a result, it is not able to perform interference cancellation or interference alignment. However, with negative correlation, a transmitter's power to favor one receiver over the other improves (in terms of the number of independent linear combinations received). This in turn enables the transmitters to perform interference alignment and interference cancellation more efficiently. When all channels are distributed independently and identically across time and space, the capacity is given by $\mathcal{C}(0.5, 0, 0)$ as shown in Fig. 2 and recovers the results of [3].

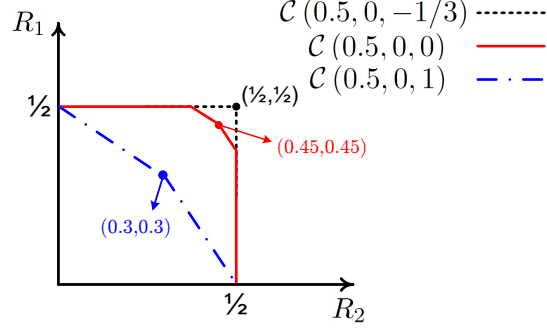


Fig. 6. Throughput region for $p = 0.5$, $\rho_{Tx} = 0$, and $\rho_{Rx} \in \{-1/3, 0, 1\}$.

To study the impact of spatial correlation at the receivers on the throughput region, we consider $\rho_{Tx} = 0$ (*i.e.* independent links at the transmitters), $\rho_{Rx} \in \{-1/3, 0, 1\}$, and $p = 0.5$. As ρ_{Rx} moves from $+1$ to -1 , the maximum achievable sum-rate improves as shown Fig. 6. For $\rho_{Rx} \in [-1, -1/3]$, $\mathcal{C}(0.5, 0, \rho_{Rx})$ includes $(R_1, R_2) = (0.5, 0.5)$ which implies that the capacity region coincides with that of instantaneous knowledge. Intuitively, negative spatial correlation at the receivers separates the signal subspace from the interference subspace which results in higher network throughput, see Section V for more details.

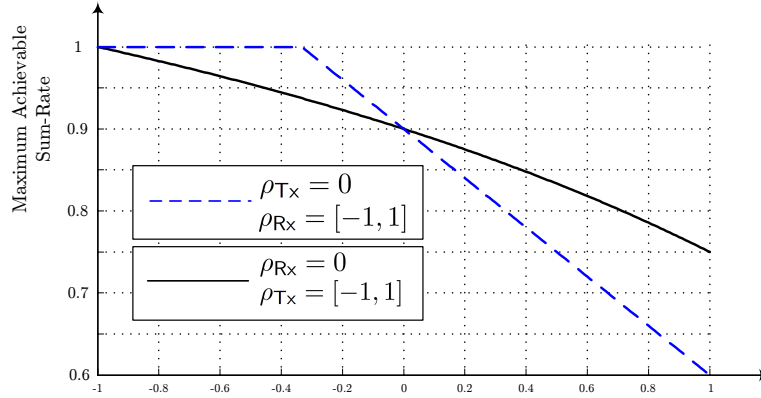


Fig. 7. The impact of spatial correlation at the transmitter side or at the receiver side on the maximum achievable sum-rate for $p = 0.5$.

To better visualize the impact of spatial correlation at the transmitters and at the receivers on the throughput region, we plot the maximum achievable sum-rate in Fig. 7 for two different scenarios with $p = 0.5$. First, we set ρ_{Tx} to be zero (dashed blue line), *i.e.* independent links at the transmitters. In this case, we see that the impact of ρ_{Rx} is linear on the maximum achievable sum-rate and it saturates at 1. Then, we set ρ_{Rx} to be zero (solid black line), *i.e.* independent links at the receivers. As we see, the impact of ρ_{Tx} is non-linear. As mentioned before, ρ_{Tx} determines the slope of the outer-bounds and thus defines the shape of the throughput region, and ρ_{Rx} defines the size of the throughput region. These arguments will be made mathematically precise in the following sections.

IV. CONVERSE PROOF OF THEOREM 1: AN EXTREMAL RANK-RATIO INEQUALITY FOR SPATIALLY CORRELATED CHANNELS

The derivation of the bounds on individual rates is straightforward and thus omitted. To derive the other bounds, we first present an extremal rank-ratio lemma tailored to spatially correlated channels.

Lemma 1 (Extremal Rank-Ratio Inequality for Spatially Correlated Channels). *For the spatially correlated interference packet network as described in Section II and for a non-zero $p \in \mathcal{S}_{\rho_{Tx}} \cap \mathcal{S}_{\rho_{Rx}}$, we have*

$$\mathbb{E} [\text{rank} [\mathbf{G}_{12}^n \mathbf{V}_1^n]] \geq \frac{1}{\beta(p, \rho_{Tx})} \mathbb{E} [\text{rank} [\mathbf{G}_{11}^n \mathbf{V}_1^n]]. \quad (22)$$

where β is given in (21).

Proof.

$$\begin{aligned} & \mathbb{E} [\text{rank} [\mathbf{G}_{12}^n \mathbf{V}_1^n]] \\ &= \mathbb{E} \left[\sum_{t=1}^n \text{rank} [\mathbf{G}_{12}^t \mathbf{V}_1^t] - \text{rank} [\mathbf{G}_{12}^{t-1} \mathbf{V}_1^{t-1}] \right] \\ &= \mathbb{E} \left[\sum_{t=1}^n \mathbf{1} \{ \alpha_{12}(t) g_{12}(t) \vec{v}_1(t) \notin \text{rowspan} (\mathbf{G}_{12}^{t-1} \mathbf{V}_1^{t-1}) \} \right] \\ &\stackrel{(a)}{=} p \mathbb{E} \left[\sum_{t=1}^n \mathbf{1} \{ g_{12}(t) \vec{v}_1(t) \notin \text{rowspan} (\mathbf{G}_{12}^{t-1} \mathbf{V}_1^{t-1}) \} \right] \\ &\stackrel{a.s.}{=} p \mathbb{E} \left[\sum_{t=1}^n \mathbf{1} \{ \vec{v}_1(t) \notin \text{rowspan} (\mathbf{G}_{12}^{t-1} \mathbf{V}_1^{t-1}) \} \right] \\ &\stackrel{(b)}{\geq} p \mathbb{E} \left[\sum_{t=1}^n \mathbf{1} \left\{ \vec{v}_1(t) \notin \text{rowspan} \begin{bmatrix} \mathbf{G}_{12}^{t-1} \mathbf{V}_1^{t-1} \\ \mathbf{G}_{11}^{t-1} \mathbf{V}_1^{t-1} \end{bmatrix} \right\} \right] \\ &\stackrel{(c)}{=} \frac{p}{2p - pq\rho_{Tx} - p^2} \mathbb{E} \left[\sum_{t=1}^n \text{rank} \begin{bmatrix} \mathbf{G}_{12}^t \mathbf{V}_1^t \\ \mathbf{G}_{11}^t \mathbf{V}_1^t \end{bmatrix} - \text{rank} \begin{bmatrix} \mathbf{G}_{12}^{t-1} \mathbf{V}_1^{t-1} \\ \mathbf{G}_{11}^{t-1} \mathbf{V}_1^{t-1} \end{bmatrix} \right] \\ &\stackrel{(d)}{=} \frac{1}{2 - \rho_{Tx} - p(1 - \rho_{Tx})} \mathbb{E} [\text{rank} [\mathbf{G}_{12}^n \mathbf{V}_1^n]] \\ &\geq \frac{1}{\beta(p, \rho_{Tx})} \mathbb{E} [\text{rank} [\mathbf{G}_{11}^n \mathbf{V}_1^n]], \\ &\geq \frac{1}{\beta(p, \rho_{Tx})} \mathbb{E} [\text{rank} [\mathbf{G}_{11}^n \mathbf{V}_1^n]], \end{aligned} \quad (23)$$

where (a) holds since $\alpha_{12}(t)$ follows a Bernoulli $\mathcal{B}(p)$ distribution; (b) follows the fact that adding $\mathbf{G}_{11}^{t-1} \mathbf{V}_1^{t-1}$ enlarges the rowspan; (c) holds since

$$\Pr(\alpha_{12}(t) = \alpha_{11}(t) = 0) = p_{ij}^{Tx} = 2p - pq\rho_{Tx} - p^2; \quad (24)$$

(d) holds since $p \neq 0$. □

The value of $\beta(p, \rho_{Tx})$ determines the ability of each transmitter to differentiate receivers in terms of number of linearly independent equations it can provide them: $\beta(p, \rho_{Tx}) = 1$ means the receivers are identical from the perspective of each transmitter and $\beta(p, \rho_{Tx}) > 1$ provides *spatial diversity* meaning that each transmitter can favor one receiver to the other. Fig. 8 illustrates $\beta(p, \rho_{Tx})$ as a function of ρ_{Tx} for $p = 3/4, 1/2, 1/4$. We observe that negative values of ρ_{Tx} increases $\beta(p, \rho_{Tx})$ and this observation is consistent with the fact that negative ρ_{Tx} results in higher network throughput as it increases the ability of transmitters to perform interference alignment.

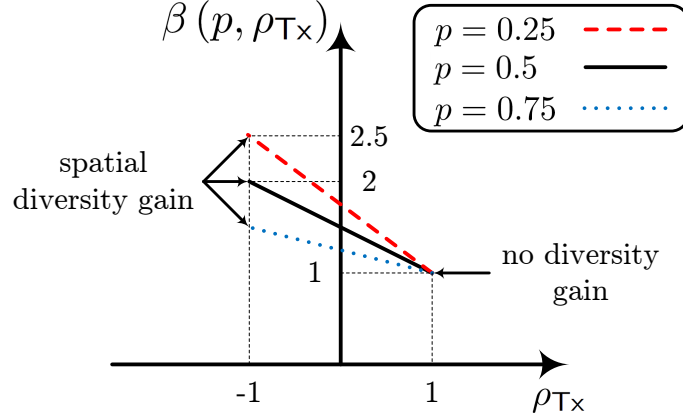


Fig. 8. Negative values of ρ_{Tx} increases $\beta(p, \rho_{Tx})$ and the ability of transmitters to perform interference alignment.

Using Lemma 1, we have

$$\begin{aligned}
 & n(R_1 + \beta(p, \rho_{Tx}) R_2) \\
 & \stackrel{a.s.}{=} \mathbb{E}[\dim(\text{Proj}_{\mathcal{I}_1^c} \text{colspan}(\mathbf{G}_{11}^n \mathbf{V}_1^n))] + \beta(p, \rho_{Tx}) \mathbb{E}[\dim(\text{Proj}_{\mathcal{I}_2^c} \text{colspan}(\mathbf{G}_{22}^n \mathbf{V}_2^n))] \\
 & \stackrel{(a)}{\leq} \mathbb{E}[\text{rank}[\mathbf{G}_{11}^n \mathbf{V}_1^n]] + \beta(p, \rho_{Tx}) \mathbb{E}[\text{rank}[\mathbf{G}_{12}^n \mathbf{V}_1^n + \mathbf{G}_{22}^n \mathbf{V}_2^n]] - \beta(p, \rho_{Tx}) \mathbb{E}[\text{rank}[\mathbf{G}_{12}^n \mathbf{V}_1^n]] \\
 & \stackrel{\text{Lemma 1}}{\leq} \beta(p, \rho_{Tx}) \mathbb{E}[\text{rank}[\mathbf{G}_{12}^n \mathbf{V}_1^n + \mathbf{G}_{22}^n \mathbf{V}_2^n]] \\
 & \stackrel{(b)}{\leq} n\beta(p, \rho_{Tx}) (1 - p_{00}^{Rx}),
 \end{aligned} \tag{25}$$

where the first equality is needed to guarantee (19) holds and each receiver can decode its intended packets; (a) follows since we ignored interference at R_{X1} ; and (b) holds since R_{X2} does not receive any useful information p_{00}^{Rx} fraction of the time.

Dividing both sides of (25) by n and let $n \rightarrow \infty$, we get

$$R_1 + \beta(p, \rho_{Tx}) R_2 \leq \beta(p, \rho_{Tx}) (1 - p_{00}^{Rx}). \tag{26}$$

Similarly, we can obtain

$$\beta(p, \rho_{Tx}) R_1 + R_2 \leq \beta(p, \rho_{Tx}) (1 - p_{00}^{Rx}). \tag{27}$$

This completes the converse proof of Theorem 1 and in the following section, we present our communication protocol.

Remark 2. The outer-bound obtained in (26) is not always active. For instance as discussed in Section III and depicted in Fig. 6, for $p = 0.5$, $\rho_{Tx} = 0$, and $\rho_{Rx} \in [-1, -1/3]$, the throughput region is determined by the bounds on individual rates, i.e. $0 \leq R_1, R_2 \leq 0.5$.

As discussed in this section, the shape of the region is defined by $\beta(p, \rho_{Tx})$ which is a function of spatial correlation at the transmitters. Spatial correlation at the receivers plays an important role as well. A positive ρ_{Rx} pulls the signal subspace and the interference subspace closer to each other while a negative ρ_{Rx} pushes them away from each other. Fig. 9 illustrates the available subspace at receiver R_{X1} for $p = 0.5$ and $\rho_{Rx} = -1, 0, 1$. For independent links at receivers $\rho_{Rx} = 0$ as in Fig. 9(a), the signal subspace and the interference subspace overlap and $1/4$ of the available subspace to receiver R_{X1} does not provide any useful information (this is when $\alpha_{11}(t) = \alpha_{21}(t) = 0$). When the links connected to R_{X1} are fully correlated, i.e. $\rho_{Rx} = 1$, the signal subspace and the interference subspace completely overlap and $1/2$ of the available subspace to receiver R_{X1} does not provide any useful information as illustrated in Fig. 9(b). Finally when $\rho_{Rx} = -1$ as in Fig. 9(c), the signal subspace and the interference subspace are completely disjoint and the entire available subspace to receiver R_{X1} is utilized. In

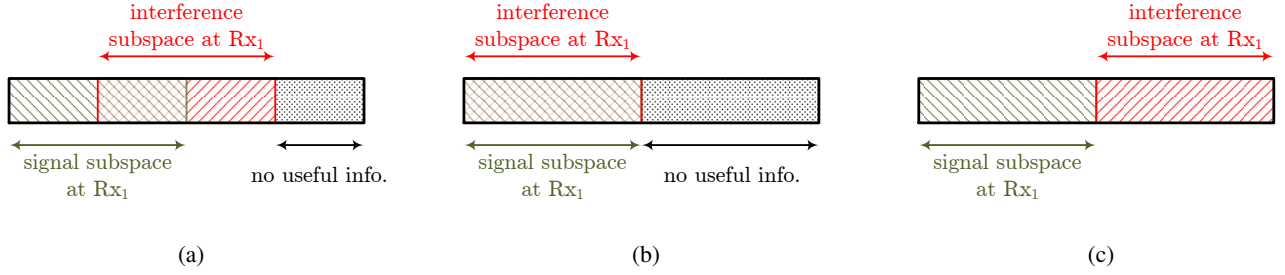


Fig. 9. The available subspace at receiver Rx_1 for $p = 0.5$ and: (a) $\rho_{Rx} = 0$; (b) $\rho_{Rx} = 1$; (c) $\rho_{Rx} = -1$. A negative ρ_{Rx} pushes the signal subspace and the interference subspace away from each other.

this latter case since interference lies in a separate subspace from the signal, the task of interference management becomes simpler and the network throughput improves.

V. ACHIEVABILITY PROOF OF THEOREM 1: COMMUNICATION PROTOCOLS FOR SPATIALLY CORRELATED PACKET NETWORKS

In this section we describe an opportunistic communication protocol (or achievability strategy) that matches the outer-bounds, thus completing the proof of Theorem 1.

We first present two examples to clarify the key ideas of the communication protocol. These examples demonstrate the impact of (positive and negative) spatial correlation at both the receiver side and the transmitter side. As we mentioned in Remark 1, fixing p , ρ_{Tx} , and ρ_{Rx} does not specify a unique channel but rather a family of channels. An interesting aspect of our communication protocol is that it only relies on the correlation coefficients rather than specific channel realizations and works for all channels within a given family.

The throughput region for spatially independent channels ($\rho_{Tx} = 0$ and $\rho_{Rx} = 0$) is given in [4]. Our communication protocol is the generalization of that result to spatially correlated channels. As we describe the protocol for the two examples, we also highlight the differences between our protocol and the communication protocol of [4]. Once the required modifications are described and justified, same changes can be applied to for any choice of p , ρ_{Tx} , and ρ_{Rx} as discussed at the end of this section.

A. Example 1: Communication Protocol for $p = \rho_{Tx} = \rho_{Rx} = 0.5$

In this example we assume that the wireless links both at the transmitters and at the receivers are positively correlated, and we present the achievability strategy for the maximum symmetric sum-rate point given by

$$\left. \frac{2\beta(p, \rho_{Tx})(1 - p_{00}^{Rx})}{1 + \beta(p, \rho_{Tx})} \right|_{p=\rho_{Tx}=\rho_{Rx}=0.5} = \frac{25}{36}. \quad (28)$$

Suppose each transmitter wishes to communicate m packets to its intended receiver. It suffices to show that this task can be accomplished (with vanishing error probability as $m \rightarrow \infty$) in

$$\left. \frac{1 + \beta(p, \rho_{Tx})}{\beta(p, \rho_{Tx})(1 - p_{00}^{Rx})} \right|_{p=\rho_{Tx}=\rho_{Rx}=0.5} m + \mathcal{O}\left(m^{\frac{2}{3}}\right) = \frac{72}{25}m + \mathcal{O}\left(m^{\frac{2}{3}}\right) \quad (29)$$

time instants. The protocol is divided into two phases described below.

Phase 1: At the beginning of the communication block, we assume that the m packets at Tx_i are in a queue² denoted by $Q_{i \rightarrow i}$, $i = 1, 2$. At each time instant t , Tx_i transmits a packet from $Q_{i \rightarrow i}$ and this packet will either stay in this initial queue or will transition to one of the queues listed in Fig. 10 for Tx_1 and \vec{a} . If at time instant t , $Q_{i \rightarrow i}$ is empty, then Tx_i , $i = 1, 2$, remains silent until the end of Phase 1.

(A) $Q_{i \rightarrow F}$: The packets for which no retransmission is required and thus we consider delivered. It is worth mentioning that any interference from Tx_i at Rx_i will be resolved by that transmitter as we describe later;

²We assume that the queues are column vectors and packets are placed in each queue according to the order they join the queue.

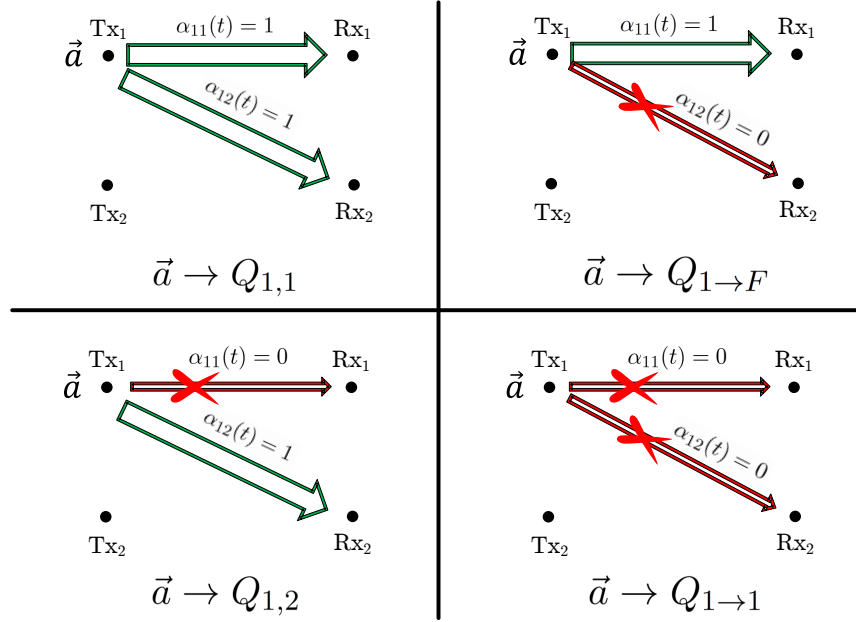


Fig. 10. Based on the shadowing coefficients at the time of communication, the status of packet \vec{a} is updated. We note that the shadowing coefficients are learned with unit delay.

- (B) $Q_{i,1}$: The packets for which at the time of communication both shadowing coefficients of the links connected to Tx_i were equal to 1;
- (C) $Q_{i,2}$: The packets for which at the time of communication we have $\alpha_{ii}(t) = 0$ and $\alpha_{i\bar{i}}(t) = 1$.

For $p = 0.5$ and $\rho_{\text{Tx}} = \rho_{\text{Rx}} = 0.5$, we have

$$\begin{aligned} p_{11}^{\text{Tx}} &= p_{11}^{\text{Rx}} = \frac{3}{8}, \\ p_{01}^{\text{Tx}} &= p_{10}^{\text{Tx}} = p_{01}^{\text{Rx}} = p_{10}^{\text{Rx}} \frac{1}{8}, \\ p_{00}^{\text{Tx}} &= p_{00}^{\text{Rx}} = \frac{3}{8}, \end{aligned} \quad (30)$$

where the notation is defined in (12) and (13). Phase 1 continues for

$$\frac{1}{1 - p_{00}^{\text{Tx}}} m + m^{\frac{2}{3}} = \frac{8}{5} m + m^{\frac{2}{3}} \quad (31)$$

time instants and if at the end of this phase either of the queues $Q_{i \rightarrow i}$ is not empty, we declare error type-I and halt the transmission (for simplicity, we assume m is chosen such that $m^{\frac{2}{3}} \in \mathbb{Z}$).

Comparison to the communication protocol for independent links: Here, spatial correlation at the transmitter side changes the length of Phase 1. For $\rho_{\text{Tx}} = 0$, we have $p_{00}^{\text{Tx}} = (1 - p)^2 = 1/4$.

Assuming that the transmission is not halted, let $N_{i,1}$ and $N_{i,2}$ denote the number of packets in queues $Q_{i,1}$ and $Q_{i,2}$ respectively at the end of the first phase, $i = 1, 2$. The transmission strategy will be halted and error type-II occurs, if any of the following events happens.

$$\begin{aligned} N_{i,1} &> \mathbb{E}[N_{i,1}] + 2m^{\frac{2}{3}} \triangleq n_{i,1}, \quad i = 1, 2; \\ N_{i,2} &> \mathbb{E}[N_{i,2}] + 2m^{\frac{2}{3}} \triangleq n_{i,2}, \quad i = 1, 2. \end{aligned} \quad (32)$$

From basic probability, we have

$$\mathbb{E}[N_{i,1}] = \frac{p_{11}^{\text{Tx}} m}{1 - p_{00}^{\text{Tx}}} = \frac{3}{5} m, \quad \mathbb{E}[N_{i,2}] = \frac{p_{01}^{\text{Tx}} m}{1 - p_{00}^{\text{Tx}}} = \frac{1}{5} m. \quad (33)$$

At the end of Phase 1, we add deterministic packets (if necessary) in order to make queues $Q_{i,1}$ and $Q_{i,2}$ of size equal to $n_{i,1}$ and $n_{i,2}$ respectively as given above, $i = 1, 2$.

Statistically a fraction

$$\frac{p_{01}^{\text{Rx}}}{p} = \frac{1}{4} \quad (34)$$

of the packets in $Q_{i,1}$ and the same fraction of the bits in $Q_{i,2}$ are known to $\text{Rx}_{\bar{i}}$, $i = 1, 2$. Denote the number of bits in $Q_{i,j}$ known to $\text{Rx}_{\bar{i}}$ by

$$N_{i,j|\text{Rx}_{\bar{i}}}, \quad i, j \in \{1, 2\}. \quad (35)$$

At the end of communication, if we have

$$N_{i,j|\text{Rx}_{\bar{i}}} < \frac{p_{01}^{\text{Rx}}}{p} n_{i,j} - 2m^{\frac{2}{3}} = \frac{1}{4} n_{i,j} - 2m^{\frac{2}{3}}, \quad i, j \in \{1, 2\}, \quad (36)$$

we declare error type-III.

Using Bernstein inequality [34], we can show that the probability of errors of types I, II, and III decreases and approaches exponentially to zero as $m \rightarrow \infty$. In fact, throughout this section, we intentionally picked $m^{\frac{2}{3}}$ to add to the constants in order to guarantee that the error terms vanish as m increases. We refer the reader to [4] for a more detailed discussion on using Bernstein inequality to analyze the error probabilities. For the rest of this subsection, we assume that Phase 1 is completed and no error has occurred.

Intuition: At this point it is worth describing the logic behind the following phase. The value of wireless is simultaneous communication to many nodes. Thus, the goal is to create linear combinations of packets that are of interest to *both* receivers.

Phase 2: During this phase we deliver sufficient number of linearly independent combinations of packets to each receiver so that they can decode their corresponding packets. A linear combination of packets is the bitwise modulo summation of the corresponding codewords in the binary field. We create these linear combinations in such a way that they are of interest to both receivers. Denote by $Q_{1,1}^c$ and $Q_{1,2}^c$ the fraction of the packets in $Q_{1,1}$ and $Q_{1,2}$ respectively for which at the time of transmission $\alpha_{22}(t) = 1$, and by $Q_{1,1}^{nc}$ and $Q_{1,2}^{nc}$ the fraction of the packets in $Q_{1,1}$ and $Q_{1,2}$ respectively for which at the time of transmission $\alpha_{22}(t) = 0$. Similar definitions apply to $Q_{2,1}^c, Q_{2,2}^c, Q_{2,1}^{nc}$ and $Q_{2,2}^{nc}$. We have

$$\mathbb{E}[N_{i,1}^c] = \frac{9}{20}m, \quad \mathbb{E}[N_{i,2}^c] = \frac{3}{20}m, \quad i = 1, 2. \quad (37)$$

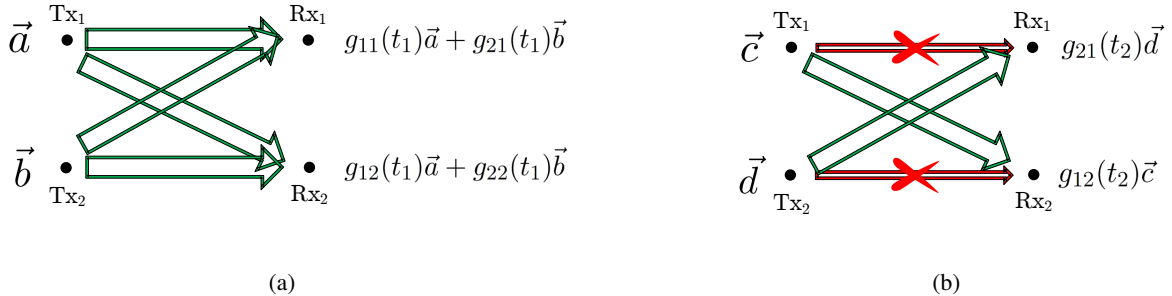


Fig. 11. Packets in $Q_{i,2}^{nc}$ can be combined with packets in $Q_{i,1}^c$ to create packets of common interest: $\vec{a} + \vec{c}$ and $\vec{b} + \vec{d}$ are of common interest to both receivers.

Packets in $Q_{i,2}^{nc}$ can be combined with packets in $Q_{i,1}^c$ to create packets of common interest as depicted in Fig. 11. Packets in $Q_{i,2}^c$ are needed at both receivers as depicted in Fig. 12 (no combination in this case). Finally, the packets in $Q_{i,1}^c$ minus the ones combined with packets in $Q_{i,2}^{nc}$ are needed at both receivers, e.g., packet \vec{a} in Fig. 11(a) is useful for both receivers. However for these remaining packets in $Q_{i,1}^c$ and $Q_{i,1}^c$ only half of them need to be

provided to both receivers. As a result, the expected number of total linearly independent combinations needed at both receivers is given by:

$$2 \times \underbrace{\frac{3}{20}m + 2}_{Q_{i,2}^c} \times \underbrace{\frac{1}{20}m}_{Q_{i,2}^{nc} \text{ combined w/ } Q_{i,1}^c} + \underbrace{\frac{8}{20}m}_{\text{remaining in } Q_{i,1}^c} = \frac{4}{5}m. \quad (38)$$

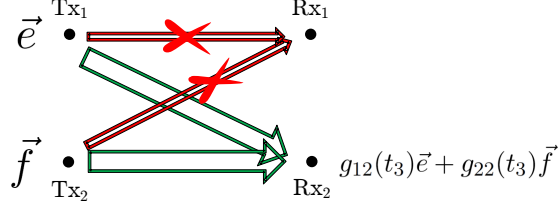


Fig. 12. Packets in $Q_{i,2}^c$ are needed at both receivers. For example, packet \vec{e} is needed at Rx_1 and helps Rx_2 to remove interference and decode its intended packet \vec{f} .

Comparison to the communication protocol for independent links: If we keep $\rho_{Tx} = 0.5$ but change ρ_{Rx} to 0 (*i.e.* independent links at the receivers), the expected number of equations needed at both receivers reduces to $3m/5$. The reason is that with $\rho_{Rx} = 0.5$ more packets are in $Q_{1,1}^c$ and $Q_{1,2}^c$ which limits the opportunity to combine packets. In other words, positive spatial correlation at receivers pushes the signal subspace and the interference subspace closer to each other which results in requiring more information to resolve interference.

We conclude that Tx_i only needs to create

$$\frac{2}{5}m + \mathcal{O}\left(m^{\frac{2}{3}}\right) \quad (39)$$

linearly independent equations of the packets in $Q_{i,1}$ and $Q_{i,2}$, $i = 1, 2$, and deliver them to *both* receivers. This problem of delivering packets to both receivers resembles a network with two transmitters and two receivers where each transmitter Tx_i wishes to communicate an independent message W_i to *both* receivers as depicted in Fig. 13, $i = 1, 2$. The channel gain model is the same as described in Section II. We refer to this problem as the two-multicast problem. It is a straightforward exercise to show that for this problem, a rate-tuple of

$$(R_1, R_2) = \left(\frac{(1 - p_{00}^{Rx})}{2}, \frac{(1 - p_{00}^{Rx})}{2} \right) = \left(\frac{5}{16}, \frac{5}{16} \right) \quad (40)$$

is achievable, see [4].

Comparison to the communication protocol for independent links: For $\rho_{Rx} = 0$ (*i.e.* independent links at the receivers), the two-multicast problem with $p = 0.5$ has a maximum achievable sum-rate of $3/4$ compared to $5/8$ for $\rho_{Rx} = 0.5$.

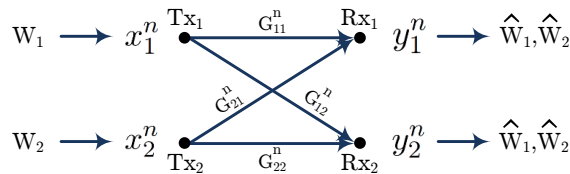


Fig. 13. Two-multicast network: Tx_i wishes to reliably communicate message W_i to both receivers, $i = 1, 2$.

Using the communication protocol of the two-multicast problem, Phase 2 lasts for

$$\underbrace{\frac{8}{5}}_{\text{one over sum-rate of 40}} \times \underbrace{\frac{4}{5}m}_{\text{\# of eqs needed}} + \mathcal{O}\left(m^{\frac{2}{3}}\right) = \frac{32}{25}m + \mathcal{O}\left(m^{\frac{2}{3}}\right) \quad (41)$$

time instants. If any error takes place, we declare error and terminate the communication. Thus to continue, we assume that the transmission is successful and no error has occurred.

Decoding: The idea is that upon completion of the communication protocol each receiver has sufficient number of linearly independent equations of the desired packets to decode them. As we described in detail, we designed the scheme in such way to guarantee this happens.

Achievable rates: Assuming that no error occurs, the total communication time is then equal to the length of Phases 1 and 2. Thus asymptotically, the total communication time is:

$$\underbrace{\frac{8}{5}m}_{\text{Phase 1}} + \underbrace{\frac{32}{25}m}_{\text{Phase 2}} + \mathcal{O}\left(m^{\frac{2}{3}}\right) = \frac{72}{25}m + \mathcal{O}\left(m^{\frac{2}{3}}\right) \quad (42)$$

time instants which is what we expected as given in (29). This completes the communication protocol for $p = 0.5$ and $\rho_{Tx} = \rho_{Rx} = 0.5$.

B. Example 2: Communication Protocol for $p = 0.45$, $\rho_{Tx} = 0$ and $\rho_{Rx} = -0.75$

This example focuses on the impact of negative spatial correlation at the receiver side and assumes independent links at the transmitters. For this particular choice of channel parameters, we can achieve

$$\left\{ \begin{array}{l} 0 \leq R_1 \leq 0.45, \\ 0 \leq R_2 \leq 0.45. \end{array} \right\} \quad (43)$$

which is maximum possible throughput regardless of the assumption on the available channel state information (since each individual link has a maximum throughput of $p = 0.45$).

The achievability strategy is divided into three phases described below compared to the two phases of the previous example.

Phase 1: This phase follows the same steps as the one introduced in the previous subsection. In this example the wireless links connected to each transmitter are uncorrelated and as a result, Phase 1 continues for

$$\frac{1}{1-q^2}m + m^{\frac{2}{3}} = \frac{1}{1-.55^2}m + m^{\frac{2}{3}} \left(\approx 1.4337m + m^{\frac{2}{3}} \right) \quad (44)$$

time instants³, and if at the end of this phase either of the queues $Q_{i \rightarrow i}$ is not empty, we declare error type-I and halt the transmission.

Phase 2: Similar to the previous example, the goal of this phase is to combine packets and use multicasting to deliver them. However, the large negative correlation at the receiver side results in fewer opportunities to combine packets. Denote by $Q_{1,1}^c$ and $Q_{1,2}^c$ the fraction of the packets in $Q_{1,1}$ and $Q_{1,2}$ respectively for which at the time of transmission $\alpha_{22}(t) = 1$, and by $Q_{1,1}^{nc}$ and $Q_{1,2}^{nc}$ the fraction of the packets in $Q_{1,1}$ and $Q_{1,2}$ respectively for which at the time of transmission $\alpha_{22}(t) = 0$. In this example $Q_{1,1}^c$ only contains a small fraction of the packets in $Q_{1,1}$. More precisely, only a fraction $p_{11}^{Rx} / (p_{10}^{Rx} + p_{11}^{Rx}) \approx 0.0376$ of the packets in $Q_{1,1}$ are placed in $Q_{1,1}^c$. We combine the packets and retransmit them similar to the previous example, and a large fraction of packets will wait for Phase 3.

Phase 3: In this phase the packets left in $Q_{1,1}^{nc}$ and $Q_{1,2}^{nc}$ are retransmitted. Since these packets are already available at the unintended receivers as shown in Fig. 11(b), they no longer create any interference when retransmitted and thus they can be delivered at a rate of $p = 0.45$ from each transmitter to its intended receiver.

³Numbers are rounded in this example.

Achievable rates: We skip decoding for this example and we just calculate the overall throughput. The total communication time is equal to:

$$\begin{aligned}
 & \underbrace{\frac{1}{1-q^2}m}_{\text{Phase 1}} + \underbrace{\frac{pp_{11}^{\text{Rx}}}{p_{10}^{\text{Rx}} + p_{11}^{\text{Rx}}} \left(1 + p + \frac{pp_{11}^{\text{Rx}}}{p_{10}^{\text{Rx}} + p_{11}^{\text{Rx}}}\right)m}_{\text{Phase 2}} \\
 & + \underbrace{\frac{qm}{1-q^2} - \left(1 - \frac{p_{11}^{\text{Rx}}}{p_{10}^{\text{Rx}} + p_{11}^{\text{Rx}}}\right)m}_{\text{Phase 3}} + \mathcal{O}\left(m^{\frac{2}{3}}\right) = \frac{20}{9}m + \mathcal{O}\left(m^{\frac{2}{3}}\right), \tag{45}
 \end{aligned}$$

which immediately implies that an overall throughput of $2p = 0.9$ is achievable in this example ($p = 0.45$, $\rho_{\text{Tx}} = 0$ and $\rho_{\text{Rx}} = -0.75$).

Comparison to the communication protocol for independent links: As mentioned before, a negative ρ_{Rx} pushes the signal subspace and the interference subspace away from each other. In this example we have $\rho_{\text{Rx}} = -0.75$ and as a result, most of the packets that arrive at the unintended receiver do not cause any interference. Since these packets are known at the unintended receiver, retransmission can be accomplished at the maximum point-to-point rate of $p = 0.45$. In this example we could not create many packets of common interest which sounds discouraging. However, since the signal and the interference subspaces are nicely separated, we could achieve the maximum possible rates.

C. Communication Protocol for General p , ρ_{Tx} and ρ_{Rx}

The communication protocol for spatially independent links, *i.e.* $\rho_{\text{Tx}} = 0$ and $\rho_{\text{Rx}} = 0$, is presented in [4] and in essence, our communication protocol builds upon that result with careful modifications to incorporate spatial correlation. Intuitively, spatial correlation at the transmitters and at the receivers affect the communication protocol in the following ways:

- 1) Spatial correlation at the transmitters (ρ_{Tx}) affects the length of Phase 1: positive correlation increases the length of Phase 1 whereas negative correlation decreases it. Moreover, ρ_{Tx} changes the distribution of packets in the queues of Fig. 10: positive correlation increases the number of packets in $Q_{1,1}$ whereas negative correlation increases the number of packets in $Q_{1,2}$. The size of these queues define the mixing procedure of the following communication phases;
- 2) Spatial correlation at the receivers (ρ_{Rx}) affects the number of interfering packets: positive correlation increases the number of packets in $Q_{1,1}^c$ and $Q_{1,2}^c$ whereas negative correlation decreases this number. In other words, a positive ρ_{Rx} pushes the signal subspace and the interference subspace closer to each other while a negative ρ_{Rx} pushes them away from each other. Moreover, ρ_{Rx} directly affects the throughput of the two-multicast problem of Fig. 13: positive correlation decreases the throughput whereas negative correlation increases the throughput.

Now that we understand intuitively how spatial correlation affects the communication protocol, consider a spatially correlated network with p , ρ_{Tx} , and ρ_{Rx} . In general, at each time the network can be in any of the 16 possible realizations of Fig. 14 where state k may occur with probability $0 \leq p_{S_k} \leq 1$, $\sum_{k=1}^{16} p_{S_k} = 1$, $k = 1, 2, \dots, 16$. In the two examples we presented above, the communication protocol at each transmitter relies on the delayed knowledge of the links connected to it and the statistics of the links connected to the other transmitter, see Fig. 10. But since at each time transmitters know all the past channel realizations, rather than relying on statistics we can use this knowledge to form the queues as described below.

- $Q_{1,1}^c$: A packet from transmitter Tx_1 moves to queue $Q_{1,1}^c$ if at the time of transmission the channel realization is S_k for $k \in \{1, 2\}$. For Tx_2 and queue $Q_{2,1}^c$ this transition happens when $k \in \{1, 3\}$;
- $Q_{1,1}^{nc}$: A packet from transmitter Tx_1 moves to queue $Q_{1,1}^{nc}$ if at the time of transmission the channel realization is S_k for $k \in \{6, 8\}$. For Tx_2 and queue $Q_{2,1}^{nc}$ this transition happens when $k \in \{10, 12\}$;
- $Q_{i,2}^c$: The status of a packet from transmitter Tx_1 is updated to $Q_{i,2}^c$ if at the time of transmission the channel realization is S_k for $k \in \{11, 12\}$. For Tx_2 and $Q_{2,2}^c$ the transition happens if $k \in \{7, 8\}$;
- $Q_{i,2}^{nc}$: The status of a packet from transmitter Tx_1 is updated to $Q_{i,2}^{nc}$ if at the time of transmission the channel realization is S_k for $k \in \{14, 15\}$. For Tx_2 and $Q_{2,2}^{nc}$ the transition happens if $k \in \{13, 15\}$.

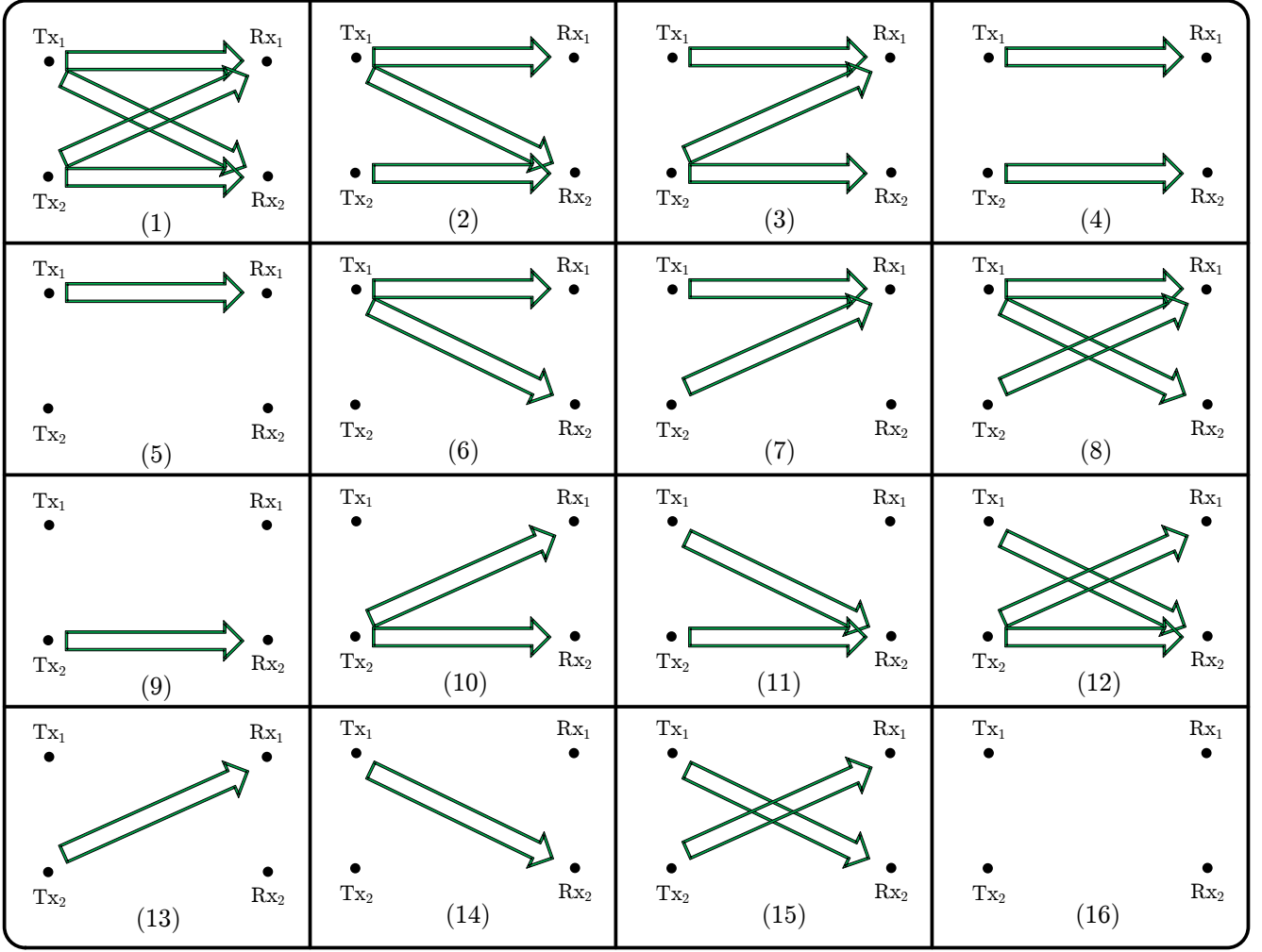


Fig. 14. At each time the network can be in any of the 16 possible realizations. The probability of each state is in agreement with p , ρ_{Tx} , and ρ_{Rx} . Only active links are depicted and if an arrow from Tx_i to Rx_j is missing, it means that link is off.

In the two examples we provided in this section, we relied on the statistics of the wireless links to form $Q_{i,1}^c$, $Q_{i,1}^{nc}$, $Q_{i,2}^c$, and $Q_{i,2}^{nc}$ but since global CSIT is available, we can actually perform this task by looking at the specific channel realizations as we did above. Once we have formed these queues, we combine them according to the following principles.

Packets in $Q_{i,2}^{nc}$ can be combined with packets in $Q_{i,1}^c$ to create packets of common interest as depicted in Fig. 11. Packets in $Q_{i,2}^c$ are needed at both receivers as depicted in Fig. 12 (no combination in this case). If after combining the packets $Q_{i,1}^c$ is not empty, such packets are useful for both receivers, *e.g.*, packet \vec{a} in Fig. 11(a). Moreover, for the remaining packets in $Q_{i,1}^c$ and $Q_{i,1}^{nc}$ only half of them need to be provided to both receivers. We communicated the combined packets and half the remaining packets in $Q_{i,1}^c$ using the transmission strategy of the two-multicast problem depicted in Fig. 13. On the other hand, suppose after combining the packets queues $Q_{1,1}^{nc}$ and $Q_{1,2}^{nc}$ are not empty. Such packets are already available at the unintended receivers as shown in Fig. 11(b) and they no longer create any interference when retransmitted and thus they can be delivered at a rate of p from each transmitter to its intended receiver. The other corner points of the capacity region can be achieved applying the same modification principles to the protocol presented in [4].

VI. CONNECTION TO OTHER PROBLEMS

In this section we describe the connections between our results and two other well-known problems.

A. Wireless Networks with Alternating Topology

Wireless networks with alternating topology were studied in [4] where each link could be on or off with some probability and capacity results were obtained for the case of instantaneous and delayed channel state information at the transmitters. Other results have considered the Degrees of Freedom of networks with alternating topology as well [35].

The shadowing coefficients $\alpha_{ij}(t)$'s in our work are designed to capture the relative strength of different signals. However, these coefficients can be interpreted as connectivity coefficients and thus, our work is closely related to the results on networks with alternating topology.

B. Wireless Packet Networks

In the context of wireless packet networks it is known that when collision occurs, the receiver can still store its analog received signal and utilize it for decoding the packets in the future. This can be done via a variety of techniques studied in multi-user joint detection and interference cancellation for cellular networks (*e.g.*, [36]–[40]). ZigZag decoding [41] also demonstrates that interference decoding and successive interference cancellation can be accomplished in 802.11 MAC. ZigZag decoding is carried on from the perspective of one receiver and takes advantage of asynchronous communication. In contrast, our work considers a network with multiple receivers and the goal is to maximize the overall network throughput. This is solely done through the knowledge of past interference pattern and no data communication between the transmitters happen. Finally, we assumed that packets are perfectly synchronized and this takes away the gain of ZigZag decoding from our problem.

VII. CONCLUSION

We studied the throughput region of spatially correlated interference packet networks. We quantified the impact of spatial correlation at the transmitters by deriving an extremal rank-ratio inequality. To achieve the outer-bounds, we developed a new transmission protocol that could have as many as three phases of communication. Our communication protocol takes full advantage of delayed interference structure knowledge and the available spatial correlation side information. We learned that spatial correlation at the transmitters defines the shape of the throughput region while spatial correlation at the receivers defines the size of this region.

In this work we assumed that each transmitter starts with a large number of packets to communicate. An interesting direction is to study and to characterize the throughput region for stochastic packet arrival with potential delivery deadlines.

REFERENCES

- [1] A. Vahid and R. Calderbank, "When does spatial correlation add value to delayed channel state information?," in *IEEE International Symposium on Information Theory (ISIT)*, pp. 2624–2628, IEEE, 2016.
- [2] N. Abramson, "The ALOHA system: another alternative for computer communications," in *Proceedings of the November 17-19, 1970, fall joint computer conference*, pp. 281–285, ACM, 1970.
- [3] A. Vahid, M. A. Maddah-Ali, and A. S. Avestimehr, "Communication through collisions: Opportunistic utilization of past receptions," in *INFOCOM*, pp. 2553–2561, IEEE, 2014.
- [4] A. Vahid, M. A. Maddah-Ali, and A. S. Avestimehr, "Capacity results for binary fading interference channels with delayed CSIT," *IEEE Transactions on Information Theory*, vol. 60, no. 10, pp. 6093–6130, 2014.
- [5] A. Vahid and R. Calderbank, "Two-user erasure interference channels with local delayed CSIT," *IEEE Transactions on Information Theory*, vol. 62, no. 9, pp. 4910–4923, 2016.
- [6] K. Jolfaei, S. Martin, and J. Mattfeldt, "A new efficient selective repeat protocol for point-to-multipoint communication," in *IEEE International Conference on Communications (ICC'93)*, vol. 2, pp. 1113–1117, IEEE, 1993.
- [7] A. F. Dana and B. Hassibi, "The capacity region of multiple input erasure broadcast channels," in *IEEE International Symposium on Information Theory (ISIT)*, pp. 2315–2319, IEEE, 2005.
- [8] L. Georgiadis and L. Tassiulas, "Broadcast erasure channel with feedback-capacity and algorithms," in *Workshop on Network Coding, Theory, and Applications (NetCod'09)*, pp. 54–61, IEEE, 2009.
- [9] J. K. Sundararajan, D. Shah, and M. Médard, "ARQ for network coding," in *IEEE International Symposium on Information Theory (ISIT)*, pp. 1651–1655, IEEE, 2008.
- [10] C.-C. Wang, "On the capacity of 1-to- k broadcast packet erasure channels with channel output feedback," *IEEE Transactions on Information Theory*, vol. 58, no. 2, pp. 931–956, 2012.
- [11] M. A. Maddah-Ali and D. Tse, "Completely stale transmitter channel state information is still very useful," *IEEE Transactions on Information Theory*, vol. 58, no. 7, pp. 4418–4431, 2012.

- [12] A. Vahid, M. A. Maddah-Ali, and A. S. Avestimehr, "Approximate capacity region of the MISO broadcast channels with delayed CSIT," *IEEE Transactions on Communications*, vol. 64, no. 7, pp. 2913–2924, 2016.
- [13] M. J. Abdoli, A. Ghasemi, and A. K. Khandani, "On the degrees of freedom of K-user SISO interference and X channels with delayed CSIT," *IEEE transactions on Information Theory*, vol. 59, no. 10, pp. 6542–6561, 2013.
- [14] A. Ghasemi, A. S. Motahari, and A. K. Khandani, "On the degrees of freedom of X channel with delayed CSIT," in *IEEE International Symposium on Information Theory Proceedings (ISIT)*, pp. 767–770, IEEE, 2011.
- [15] C. S. Vaze and M. K. Varanasi, "The degrees of freedom region and interference alignment for the MIMO interference channel with delayed CSIT," *IEEE Transactions on Information Theory*, vol. 58, no. 7, pp. 4396–4417, 2012.
- [16] H. Maleki, S. A. Jafar, and S. Shamai, "Retrospective interference alignment," in *IEEE International Symposium on Information Theory Proceedings (ISIT)*, pp. 2756–2760, 2011.
- [17] R. Tandon, S. Mohajer, H. V. Poor, and S. Shamai, "Degrees of freedom region of the MIMO interference channel with output feedback and delayed CSIT," *IEEE Transactions on Information Theory*, vol. 59, no. 3, pp. 1444–1457, 2013.
- [18] B. Nazer, M. Gastpar, S. A. Jafar, and S. Vishwanath, "Ergodic interference alignment," *IEEE Transactions on Information Theory*, vol. 58, no. 10, pp. 6355–6371, 2012.
- [19] S. Lashgari, A. S. Avestimehr, and C. Suh, "Linear degrees of freedom of the X-channel with delayed CSIT," *IEEE Transactions on Information Theory*, vol. 60, no. 4, pp. 2180–2189, 2014.
- [20] M. J. Abdoli and A. S. Avestimehr, "Layered interference networks with delayed CSI: DoF scaling with distributed transmitters," *IEEE Transactions on Information Theory*, vol. 60, no. 3, pp. 1822–1839, 2014.
- [21] A. Vahid, I. Shomorony, and R. Calderbank, "Informational bottlenecks in two-unicast wireless networks with delayed CSIT," in *53rd Annual Allerton Conference on Communication, Control, and Computing (Allerton)*, pp. 1256–1263, IEEE, 2015.
- [22] M. Kobayashi, S. Yang, D. Gesbert, and X. Yi, "On the degrees of freedom of time correlated MISO broadcast channel with delayed CSIT," in *IEEE International Symposium on Information Theory Proceedings (ISIT)*, pp. 2501–2505, IEEE, 2012.
- [23] S. Yang, M. Kobayashi, D. Gesbert, and X. Yi, "Degrees of freedom of time correlated MISO broadcast channel with delayed CSIT," *IEEE Transactions on Information Theory*, vol. 59, no. 1, pp. 315–328, 2013.
- [24] P. de Kerret, D. Gesbert, J. Zhang, and P. Elia, "Optimal sum-DoF of the K-user MISO BC with current and delayed feedback," *arXiv preprint arXiv:1604.01653*, 2016.
- [25] T. Gou and S. A. Jafar, "Optimal use of current and outdated channel state information: Degrees of freedom of the MISO BC with mixed CSIT," *IEEE Communications Letters*, vol. 16, no. 7, pp. 1084–1087, 2012.
- [26] X. Yi, S. Yang, D. Gesbert, and M. Kobayashi, "The degrees of freedom region of temporally correlated MIMO networks with delayed CSIT," *IEEE Transactions on Information Theory*, vol. 60, no. 1, pp. 494–514, 2014.
- [27] J. Chen and P. Elia, "Symmetric two-user MIMO BC with evolving feedback," in *Information Theory and Applications Workshop (ITA)*, pp. 1–5, IEEE, 2014.
- [28] V. Raghavan, S. V. Hanly, and V. V. Veeravalli, "Statistical beamforming on the grassmann manifold for the two-user broadcast channel," *IEEE Transactions on Information Theory*, vol. 59, no. 10, pp. 6464–6489, 2013.
- [29] J. Choi, V. Raghavan, and D. J. Love, "Limited feedback design for the spatially correlated multi-antenna broadcast channel," in *IEEE Global Communications Conference (GLOBECOM)*, pp. 3481–3486, IEEE, 2013.
- [30] M. Dai and B. Clerckx, "Transmit beamforming for MISO broadcast channels with statistical and delayed CSIT," *IEEE Transactions on Communications*, vol. 63, no. 4, pp. 1202–1215, 2015.
- [31] B. Clerckx and D. Gesbert, "Space-Time encoded MISO broadcast channel with outdated CSIT: An error rate and diversity performance analysis," *IEEE Transactions on Communications*, vol. 63, no. 5, pp. 1661–1675, 2015.
- [32] B. Nosrat-Makouei, J. G. Andrews, and R. W. Heath, "MIMO interference alignment over correlated channels with imperfect CSI," *IEEE Transactions on Signal Processing*, vol. 59, no. 6, pp. 2783–2794, 2011.
- [33] M. J. Wainwright, M. I. Jordan, *et al.*, "Graphical models, exponential families, and variational inference," *Foundations and Trends® in Machine Learning*, vol. 1, no. 1–2, pp. 1–305, 2008.
- [34] S. Bernstein, "On a modification of chebyshev's inequality and of the error formula of laplace," *Ann. Sci. Inst. Sav. Ukraine, Sect. Math*, vol. 1, no. 4, pp. 38–49, 1924.
- [35] H. Sun, C. Geng, and S. A. Jafar, "Topological interference management with alternating connectivity," in *Information Theory Proceedings (ISIT), 2013 IEEE International Symposium on*, pp. 399–403, IEEE, 2013.
- [36] J. Boutros and G. Caire, "Iterative multiuser joint decoding: Unified framework and asymptotic analysis," *IEEE Transactions on Information Theory*, vol. 48, no. 7, pp. 1772–1793, 2002.
- [37] S. Verdu, *Multiuser detection*. Cambridge university press, 1998.
- [38] D. Reynolds, X. Wang, and H. V. Poor, "Blind adaptive space-time multiuser detection with multiple transmitter and receiver antennas," *IEEE Transactions on Signal Processing*, vol. 50, no. 6, pp. 1261–1276, 2002.
- [39] H. El Gamal and E. Geraniotis, "Iterative multiuser detection for coded CDMA signals in AWGN and fading channels," *IEEE Journal on Selected Areas in Communications*, vol. 18, no. 1, pp. 30–41, 2000.
- [40] H. V. Poor, "Iterative multiuser detection," *Signal Processing Magazine*, vol. 21, no. 1, pp. 81–88, 2004.
- [41] S. Gollakota and D. Katabi, *Zigzag decoding: combating hidden terminals in wireless networks*, vol. 38. ACM, 2008.